Bulletin of the JSME Vol.3, No.3, 2016
Mechanical Engineering Journal

Motion optimization for first-aid chest compression based on kinematic, dynamic and temporal redundancy

Masafumi OKADA* and Shun KAYASHIMA*
* Dept. of Mechanical Sciences and Engineering, Tokyo Institute of Technology
2-12-1 Oookayama Meguro-ku Tokyo 152-8552, JAPAN
E-mail: okada@mep.titech.ac.jp

Received 4 March 2015

Abstract
The chest compression is one of the most important actions for first-aid cardio-pulmonary resuscitation (CPR). Since it requires large torque/force to be generated, the performers have to take an energy saving position and motion until advanced life support providers take over. In the basic life-saving certification, an expert demonstrates the chest compression and trainees behave like him. However, since the energy saving motion strictly depends on the body weight and height of the performers, an appropriate indication and instruction for the trainees will be necessary. In this paper, we optimize the chest compression from kinematic, dynamic and temporal point of view. By using Pseudo-differential and zero-phase filter, the angular velocity and acceleration are derived from a motion capture data, and generative force is calculated by inverse dynamic computation. Based on an evaluation function and constraints, the chest compression is optimized kinematically, dynamically and temporally. Moreover, for the chest compression of a child with light weight, a motion aid is optimized. The effectiveness of the proposed method is evaluated based on a physical load of the performers by measuring heart rate.

Key words : Chest compression, Motion optimization, Pseudo-differential and zero-phase filter, Motion aid

1. Introduction

The chest compression as shown in Fig.1 is one of the most important actions for first-aid cardio-pulmonary resuscitation (CPR). Because victims in cardio-respiratory arrest will be saved by being provided compressions as soon as possible until advanced life support providers take over, it is expected that the chest compressions is widely known in public. American Heart Association (AHA) established a guideline of the chest compressions (Field, Hazinski and

Fig. 1 First-aid chest compression

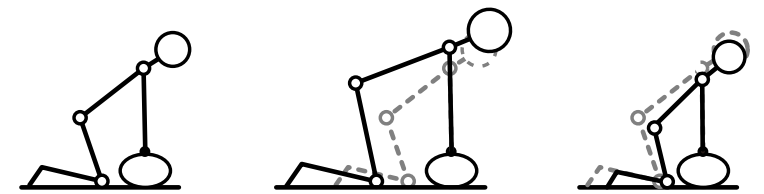

Fig. 2 The difference of the appropriate chest compression

Sayre, 2010) with a qualitative representation which is "Provide chest compressions at least 100/min to adequate depth (at least 5cm)". In the training session of CPR, an expert demonstrates the chest compression, and trainees behave like him. However, since the chest compression requires very large force and torque to be generated, an energy saving motion is necessary to continue it long time. Because the appropriateness of this motion strictly depends on the body length and weight of the performers as shown in Fig.2, it will be required to show a suitable motion to the trainees based on their

Paper No.15-00155
J-STAGE Advance Publication date: 13 April, 2016
[DOI: 10.1299/mej.15-00155]

physical body size. The purpose of this research is to obtain an optimal chest compression that minimizes the joint torques of the performer considering his body length and weight.

Many motion optimization methods have been proposed so far. For example, Hollerbach (Hollerbach and Suh, 1987) minimized manipulator's torques using kinematic redundancy. Because chest compression is a dynamic motion, dynamic optimization is required. Wang (Wang, Timoszyk and Bobrow, 2001), Kim (Kim and Park, 2008) and Kim (Kim, 2011) optimized the motion data of a manipulator from dynamic point of view. The motion is represented by a B-spline curve, and parameters are optimized so that the payload of the manipulator is maximized. Khoury (Khoury, Lamiraux and Taix 2013) proposed humanoid motion planning based on an evaluation function and constraints. The motion is represented by a polynomial. However, the motion data of the chest compression is not limited to B-spline curve or polynomial, thus another methodology that handles arbitrary curves will be required. Wang (Wang, Hammer, Delp and Koltun, 2012) generates human natural walking considering the optimization of metabolic energy based on human dynamics. This method is specialized only for walking.

On the chest compressions, some researches have been reported. Boyle (Boyle, Wilson, Connelly, McGuigan, Wilson and Whitbourn, 2002) and Abellaa (Abellaa, Edelsonb, Kim, Retzerc, Myklebustd, Barryc, O'Hearn, Vanden Hoek and Beckera, 2007) developed feedback equipment to instruct an appropriate timing and force for the performers. In particular, we developed an enhanced motion to instruct the large force to be generated (Okada and Kayashima, 2013). Our algorithm utilized a skilled chest compression, however, the appropriate motion has to be provided depending on the body parameters of the performers.

In this paper, we propose a motion optimization method for the chest compression. Since a human model of the chest compression configures a closed kinematic chain, it contains kinematic redundancy. Since the constraint of the motion is specified only by a compressing time, *i.e.* the trajectory of the motion is not specified, it contains dynamic redundancy. Since the appropriate compressing time depends on the body parameters of the performer, it contains temporal redundancy. These three redundancies are optimized based on a gradient method using an evaluate function. Moreover, a helpful motion aid for a light weight performer is also optimized. Finally, it is confirmed that the physical load of the performer is reduced by using the motion aid measuring heart rate during the chest compressions.

2. Motion optimization for arbitrary curve

2.1. Human link model

The human providing the chest compression is molded by Fig.3. Link 1, 2, 3 represent the thigh, trunk, arm whose

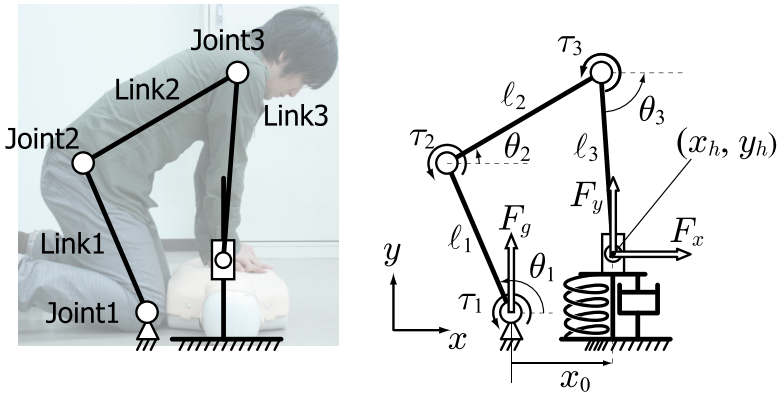

Fig. 3 Link model of human chest compression and its parameter definition

lengths are ℓ_1, ℓ_2, ℓ_3. Joint 1, 2, 3 represent the knee, hip, shoulder joint, respectively. Joint angles are defined by θ_1, θ_2 and θ_3 in absolute coordinates, joint torques are defined by τ_1, τ_2 and τ_3. The position of the hand is defined by $\boldsymbol{x}_h = (x_h,\ y_h)$. The victim is modeled by a spring and damper, and its height is same as y_h with the assumption that the performer's hand is fixed on the chest. The ground force on the knee joint is defined by F_g and the reaction force on the hand is represented by F_x and F_y. F_y is obtained by;

$$F_y = k(y_{h0} - y_h) - c\dot{y}_h \tag{1}$$

where k is a spring constant, c is a viscos coefficient and y_{h0} is a natural height of the chest. F_x is a friction force between the hand and chest. x_0 represents the distance between the performer and victim ($x_h = x_0$ will be a constraint of this model).

[DOI: 10.1299/mej.15-00155]

Based on these parameters, the dynamic equation of the human chest compression is obtained by;

$$M(\boldsymbol{\theta})\ddot{\boldsymbol{\theta}} + C(\boldsymbol{\theta}, \dot{\boldsymbol{\theta}}) + G(\boldsymbol{\theta}) = K \begin{bmatrix} \boldsymbol{\tau} \\ F_x \end{bmatrix} \tag{2}$$

$$\boldsymbol{\theta} = \begin{bmatrix} \theta_1 & \theta_2 & \theta_3 \end{bmatrix}^T, \quad \boldsymbol{\tau} = \begin{bmatrix} \tau_1 & \tau_2 & \tau_3 \end{bmatrix}^T \tag{3}$$

where M, C and G represent inertia matrix, centrifugal and Coriolis term, and gravity term, respectively. K defines the distribution of torques and force to joint actions.

2.2. Problem formulation

The purpose of this paper is to obtain the time sequence data of the joint angle and torque;

$$\Theta = \begin{bmatrix} \boldsymbol{\theta}_1 & \boldsymbol{\theta}_2 & \cdots & \boldsymbol{\theta}_N \end{bmatrix}, \quad \boldsymbol{\theta}_i = \begin{bmatrix} \theta_{1i} & \theta_{2i} & \theta_{3i} \end{bmatrix}^T \tag{4}$$

$$\boldsymbol{T} = \begin{bmatrix} \boldsymbol{\tau}_1 & \boldsymbol{\tau}_2 & \cdots & \boldsymbol{\tau}_N \end{bmatrix}, \quad \boldsymbol{\tau}_i = \begin{bmatrix} \tau_{1i} & \tau_{2i} & \tau_{3i} \end{bmatrix}^T \tag{5}$$

that minimize the objective function J;

$$J = \sum_{i=1}^{N} \left(\|W_\tau \boldsymbol{\tau}_i\|^2 + \|w_x F_{xi}\|^2 \right) \tag{6}$$

with the constraints:

$$x_{hi} = \ell_1 \cos\theta_{1i} + \ell_2 \cos\theta_{2i} + \ell_3 \cos\theta_{3i} = x_0 \tag{7}$$

$$F_{gi} > 0, \quad F_{yi} > 0 \tag{8}$$

Moreover, to realize an appropriate compression

$$y_{h1} = y_{h0} \tag{9}$$

$$y_{hn} = y_{h0} - 5\text{cm} \tag{10}$$

$$\dot{y}_{h1} = \dot{y}_{hn} = 0 \tag{11}$$

are satisfied, where n represents a specified time (compressing time), and y_{hi} is defined by:

$$y_{hi} = \ell_1 \sin\theta_{1i} + \ell_2 \sin\theta_{2i} + \ell_3 \sin\theta_{3i} \tag{12}$$

Because the hand of the performer is fixed to the chest of the victim by a friction, the smaller F_x is required in Eq. (6) for small internal force. W_τ is a constant diagonal matrix that has small value corresponding to the hip joint (the human will generate large torque in hip joint). w_x is a constant number. We remark that

$$\boldsymbol{\theta}_{N+1} = \boldsymbol{\theta}_1, \quad \boldsymbol{\tau}_{N+1} = \boldsymbol{\tau}_1 \tag{13}$$

are satisfied because the chest compression is a cyclic motion. The design parameters for the optimization are $\boldsymbol{\theta}_i$, y_{hi} $(i = 1, 2, \cdots, N)$ and x_0.

2.3. Optimization procedure

2.3.1. Kinematic and dynamic optimization Since the kinematic constraint is given by Eq. (7), that is the hand position in x coordinate, the posture of the performer has kinematic redundancy as shown in Fig.4. Moreover, the change of x_0 yields the change of posture. Thus, the optimization contains the redundancy optimization of kinematics. Since

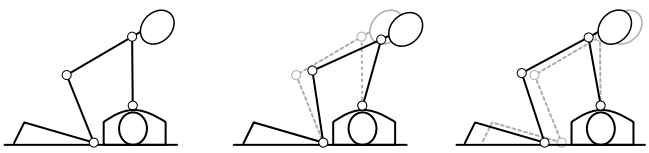

Fig. 4 Kinematic redundancy of the chest compression

Fig.4(a) configures a four-bar linkage, the initial posture has kinematic redundancy as shown in Fig.4(b). Moreover, because x_0 is changeable, it yields another posture as shown in Fig.4(c).

[DOI: 10.1299/mej.15-00155]

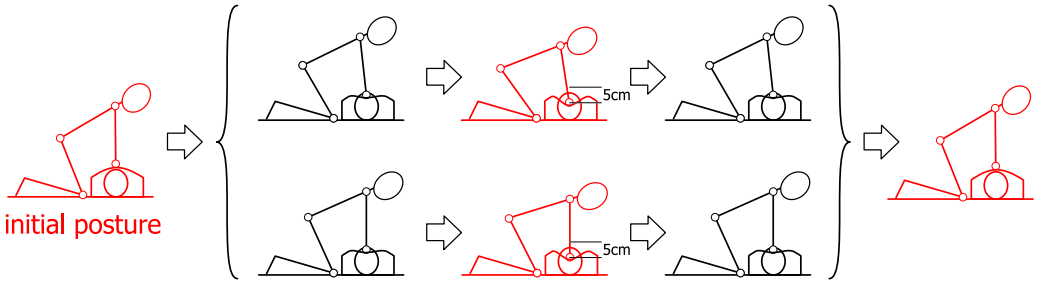

Fig. 5 Dynamical redundancy of the chest compression

On the other hand, the motion is restricted by Eqs. (9), (10) and (11) which are compression depth of initial and compressing time while the path to these postures is not specified. Thus, the optimization also contains the redundancy optimization of dynamic motion as shown in Fig.5. Even though the same initial posture, there are some paths that satisfy the constraints.

2.3.2. Temporal optimization In Eq. (10), y_{hn} is specified at specified time n. For the effective use of inertia forces, n will depend on the physical parameters on the performer (body height and weight). Thus, in the optimization procedure, n is optimized as shown in Fig.6 so that J is minimized, which is the optimization of temporal redundancy.

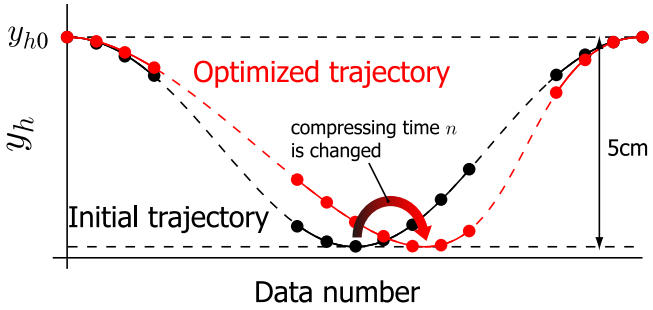

Fig. 6 Temporal redundancy of compressing time

3. Optimization method

3.1. Capturing a skilled chest compression

To obtain the initial value of Θ in Eq. (4), the skilled chest compression is motion captured. The performer is an emergency life guard from Tokyo Disaster Prediction and Emergency Medical Service Association. His weight is 69.3kg and height is 172cm.

Seven markers are set on the performer's knee, hip, shoulder, back, head, chest and hand as shown in Fig. 7. Figure 8

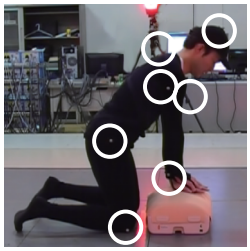

Fig. 7 Marker position

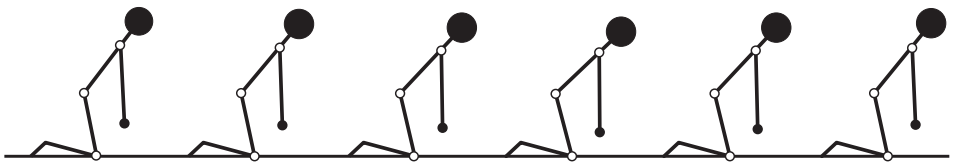

Fig. 8 Skilled chest compression (motion capture data)

shows the captured motion. The motion is small but he generates about 420N maximum from his hand which is measured by a force sensor on the floor.

3.2. Inverse dynamic analysis

Inverse dynamic analysis is performed to obtain the torque data in Eq. (5). It requires the information of $\dot{\Theta}$ and $\ddot{\Theta}$. In this paper, we calculate $\dot{\Theta}$ and $\ddot{\Theta}$ by using pseudo-differential and zero-phase filter. Consider transfer functions of

[DOI: 10.1299/mej.15-00155]

low-pass filter G^0 and pseudo-differential G^1 as:

$$G^0(s) = \frac{F}{s+F}, \quad G^1(s) = \frac{sF}{s+F} \tag{14}$$

Their impulse responses in discrete time domain are defined by;

$$\boldsymbol{g}^0 = \left\{ \begin{array}{cccc} g^0(0) & g^0(T) & \cdots & g^0((N-1)T) \end{array} \right\}, \quad \boldsymbol{g}^1 = \left\{ \begin{array}{cccc} g^1(0) & g^1(T) & \cdots & g^1((N-1)T) \end{array} \right\} \tag{15}$$

where F means a crossover frequency of the low-pass filter, T is a sampling time. Pseudo-differential and zero-phase filter gives $\dot{\Theta}$ as shown in Fig. 9. Step 1 means filtering of Θ by G^1 and $\hat{\dot{\Theta}}$ is obtained. Step 2 represents a reversing of the data

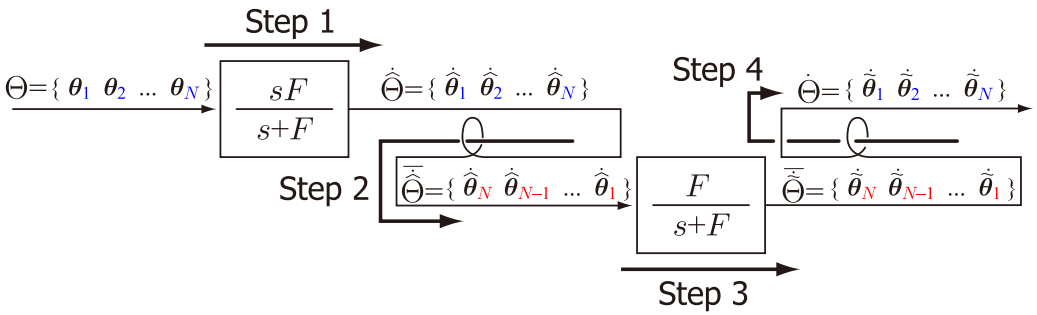

Fig. 9 Pseudo-differential and zero-phase filter

sequence, and gives $\bar{\hat{\dot{\Theta}}}$. In Step 3, $\bar{\hat{\dot{\Theta}}}$ is filtered by G^0 to cancel the phase-lag, and $\bar{\hat{\ddot{\Theta}}}$ is obtained. By reversing the data sequence of $\bar{\hat{\ddot{\Theta}}}$ once again, we obtain $\dot{\Theta}$ in Step 4. By replacing G^0 in Step 3 to $-G^1$, $\ddot{\Theta}$ is obtained by the same way.

Because the chest compression is a cyclic motion, pseudo-differential and zero-phase filtering is represented by the following calculations.

$$\dot{\Theta} = \Theta F^1, \quad F^1 = \boldsymbol{G}^1 R \boldsymbol{G}^0 R \tag{16}$$

$$\ddot{\Theta} = \Theta F^2, \quad F^2 = -\boldsymbol{G}^1 R \boldsymbol{G}^1 R \tag{17}$$

$$\boldsymbol{G}^k = \begin{bmatrix} g^k(0) & g^k((N-1)T) & \cdots & g^k(T) \\ g^k((N-1))T & g^k((N-2)T) & \cdots & g^k(0) \\ \vdots & \vdots & & \vdots \\ g^k(T) & g^k(0) & \cdots & g^k(2T) \end{bmatrix}, \quad R = \begin{bmatrix} 0 & \cdots & 0 & 1 \\ 0 & \cdots & 1 & 0 \\ \vdots & \iddots & \vdots & \vdots \\ 1 & \cdots & 0 & 0 \end{bmatrix} \tag{18}$$

Multiplication by $\boldsymbol{G}^k$ means a convolution with an impulse response, and R means reversing of the data sequence. The key point of this method is that the angular velocity and acceleration are simply represented by a multiplication of angular data and constant matrix, which enables simple calculation of $\partial\dot{\theta}/\partial\theta$ and $\partial\ddot{\theta}/\partial\theta$ in Sect. 3.4.

By using Θ, $\dot{\Theta}$ and $\ddot{\Theta}$, $\boldsymbol{\tau}$ and F_x is obtained from Eq. (2). Because the link model of human chest compression configures closed kinematic loop, *i.e.* it is an over actuated system, τ and F_x is calculated by the following equations.

$$\begin{bmatrix} \boldsymbol{T} \\ \boldsymbol{F}_x \end{bmatrix} = W^{-1}\left(KW^{-1}\right)^{\#}\left\{M(\Theta)\ddot{\Theta} + C(\Theta,\dot{\Theta}) + G(\Theta)\right\} \tag{19}$$

$$W = \begin{bmatrix} W_\tau & 0 \\ 0 & w_x \end{bmatrix} \tag{20}$$

$$\boldsymbol{F}_x = \begin{bmatrix} F_{x1} & F_{x2} & \cdots & F_{xN} \end{bmatrix} \tag{21}$$

$A^{\#}$ is a pseudo-inverse of A defined by $(A^TA)^{-1}A^T$, thus Eq. (19) minimizes Eq. (6).

3.3. Inverse kinematic analysis

Because of the closed kinematic constraint of human link model, Degree-of-freedom of the system is one. Thus, θ_2 and θ_3 are represented by the function of θ_1. By defining $\alpha, \beta, \gamma, \phi$, ℓ_4 and ℓ_5 as shown in Fig.10, the following equations are satisfied.

$$\theta_2 = \alpha + \beta - \pi + \theta_1, \quad \theta_3 = \gamma - \pi + \theta_2 \tag{22}$$

$$\ell_4 = \sqrt{x_h^2 + y_h^2}, \quad \ell_5 = \sqrt{\ell_1^2 + \ell_4^2 - 2\ell_1\ell_4\cos(\theta_1 - \phi)} \tag{23}$$

[DOI: 10.1299/mej.15-00155]

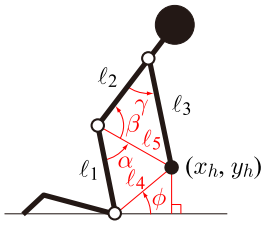

Fig. 10 Parameter definition for inverse kinematics

$$\alpha = \cos^{-1}\left(\frac{\ell_1^2+\ell_5^2-\ell_4^2}{2\ell_1\ell_5}\right), \quad \beta = \cos^{-1}\left(\frac{\ell_2^2+\ell_5^2-\ell_3^2}{2\ell_2\ell_5}\right), \quad \gamma = \cos^{-1}\left(\frac{\ell_2^2+\ell_3^2-\ell_5^2}{2\ell_2\ell_3}\right), \quad \phi = \tan^{-1}\frac{y_h}{x_h} \tag{24}$$

3.4. Gradient calculation

For the optimization of the objective function in Eq. (6), a gradient method is utilized. The gradient of J with respect to the design parameters (θ_{1i}, y_{hi} and x_0) are obtained by:

$$\nabla_{\theta_{1i}} J = \frac{\partial J}{\partial \theta_{1i}} + \frac{\partial J}{\partial \dot{\theta}_{1i}}\frac{\partial \dot{\theta}_{1i}}{\partial \theta_{1i}} + \frac{\partial J}{\partial \ddot{\theta}_{1i}}\frac{\partial \ddot{\theta}_{1i}}{\partial \theta_{1i}} + \sum_{k=2}^{3}\left(\frac{\partial J}{\partial \theta_{ki}}\frac{\partial \theta_{ki}}{\partial \theta_{1i}} + \frac{\partial J}{\partial \dot{\theta}_{ki}}\frac{\partial \dot{\theta}_{ki}}{\partial \theta_{1i}} + \frac{\partial J}{\partial \ddot{\theta}_{ki}}\frac{\partial \ddot{\theta}_{ki}}{\partial \theta_{1i}}\right) \tag{25}$$

$$\nabla_{y_{hi}} J = \sum_{k=2}^{3}\left(\frac{\partial J}{\partial \theta_{ki}}\frac{\partial \theta_{ki}}{\partial y_{hi}} + \frac{\partial J}{\partial \dot{\theta}_{ki}}\frac{\partial \dot{\theta}_{ki}}{\partial y_{hi}} + \frac{\partial J}{\partial \ddot{\theta}_{ki}}\frac{\partial \ddot{\theta}_{ki}}{\partial y_{hi}}\right) \tag{26}$$

$$\nabla_{x_0} J = \sum_{i=1}^{N}\left\{\sum_{k=2}^{3}\left(\frac{\partial J}{\partial \theta_{ki}}\frac{\partial \theta_{ki}}{\partial x_0} + \frac{\partial J}{\partial \dot{\theta}_{ki}}\frac{\partial \dot{\theta}_{ki}}{\partial x_0} + \frac{\partial J}{\partial \ddot{\theta}_{ki}}\frac{\partial \ddot{\theta}_{ki}}{\partial x_0}\right)\right\} \tag{27}$$

$\partial\theta_k/\partial\theta_1$ ($k = 2, 3$) is obtained from Eq. (22). $\partial\dot{\theta}_1/\partial\theta_1$ and $\partial\ddot{\theta}_1/\partial\theta_1$ are obtined from Eq. (16) and (17). $\partial\dot{\theta}_k/\partial\theta_1$ and $\partial\ddot{\theta}_k/\partial\theta_1$ ($k = 2, 3$) are obtained by;

$$\frac{\partial \dot{\theta}_k}{\partial \theta_1} = \frac{\partial \dot{\theta}_k}{\partial \theta_k}\frac{\partial \theta_k}{\partial \theta_1}, \quad \frac{\partial \ddot{\theta}_k}{\partial \theta_1} = \frac{\partial \ddot{\theta}_k}{\partial \theta_k}\frac{\partial \theta_k}{\partial \theta_1} \tag{28}$$

Eq. (26) utilizes Eq. (12). Eq. (27) utilizes Eqs. (7), (16), (17) and (22). Thus $\nabla_{\theta_{1i}} J$, $\nabla_{y_{hi}} J$ and $\nabla_{x_0} J$ are analytically calculated.

3.5. Satisfaction of constraints in inequality

This optimization procedure includes the constraints in Eq. (8) which are represented by inequalities. To satisfy these constraints, J_c is set as;

$$J_c = \sum_{i=1}^{N}\left(\sigma(F_{gi})F_{gi} + \sigma(F_{yi})F_{yi}\right) \tag{29}$$

$$\sigma(F) = \frac{1}{1+\exp(aF)} \tag{30}$$

and $\nabla_{\theta_{1i}} J_c$, $\nabla_{y_{hi}} J_c$ and $\nabla_{x_0} J_c$ are calculated. Because Eq. (30) represents sigmoid function with an appropriate constant a, ∇J_c has a positive value only when $F \simeq 0$.

3.6. Updating the design parameters

Based on the obtained gradients, the design parameters θ_{1i} and x_0 are updated by;

$$\theta_{1i} \leftarrow \theta_{1i} + \delta\left(w\nabla_{\theta_{1i}} J + w_c \nabla_{\theta_{1i}} J_c\right) \tag{31}$$

$$x_0 \leftarrow x_0 + \delta\left(w\nabla_{x_0} J + w_c \nabla_{x_0} J_c\right) \tag{32}$$

where w and w_c are weighting parameters, and δ is a small constant. On the other hand, Eq. (11) is a constraint of velocity $\dot{y}_h$, and the time sequence data of updated y_h has to satisfy this constraint. Same as Eq. (16), $\dot{y}_h$ is defined as;

$$\dot{Y}_h = Y_h F^1 \tag{33}$$

$$Y_h = \begin{bmatrix} y_{h1} & y_{h2} & \cdots & y_{hN} \end{bmatrix} \tag{34}$$

[DOI: 10.1299/mej.15-00155]

and $\dot{y}_h$ will be updated by:

$$\dot{Y}_h \leftarrow \dot{Y}_h + \Delta\dot{Y}_h = (Y_h + \Delta Y_h)F^1 \tag{35}$$

$$\Delta Y_h = \begin{bmatrix} \Delta y_{h1} & \Delta y_{h2} & \cdots & \Delta y_{hN} \end{bmatrix}, \quad \Delta y_{hi} = \left(w\nabla_{y_{hi}} J + w_c \nabla_{y_{hi}} J_c\right) \tag{36}$$

By considering the elemnts of $\dot{Y}_h$, Eq. (11) is rewritten by:

$$\begin{bmatrix} \dot{y}_{h1} & \dot{y}_{hn} \end{bmatrix} = \Delta Y_h F^1_{1,n} = 0 \tag{37}$$

where $F^1_{1,n}$ is defined by;

$$F^1_{1,n} = \begin{bmatrix} f^1_1 & f^1_n \end{bmatrix} \tag{38}$$

and f^1_i is an i-th column vector of F^1 as:

$$F^1 = \begin{bmatrix} f^1_1 & f^1_2 & \cdots & f^1_N \end{bmatrix} \tag{39}$$

From these considerations, ΔY_h is projected onto the constraints space, which means y_h is updated by the following equations;

$$Y_h \leftarrow Y_h + \delta\Delta\hat{Y}_h \tag{40}$$

$$\Delta\hat{Y}_h = \Delta Y_h \left\{ I - F^1_{1,n} \left(F^1_{1,n}\right)^{\#} \right\} \tag{41}$$

where I is an identity. Using Eqs. (31), (32) and (40), iteration is executed.

4. Motion optimization of chest compression

4.1. Motion capture data and optimized motion

Based on the proposed method in the previous section, the human chest compression is optimized. The lengths of each link are:

$$\ell_1 = 0.423, \quad \ell_2 = 0.429, \quad \ell_3 = 0.412 \tag{42}$$

Since the motion is captured in each 5msec ($T = 0.005$) and motion cycle is 0.6sec, number of data $N = 120$. The expert motion in Fig.8 is optimized and the result is shown in Fig.11. The black line represents the captured skilled motion

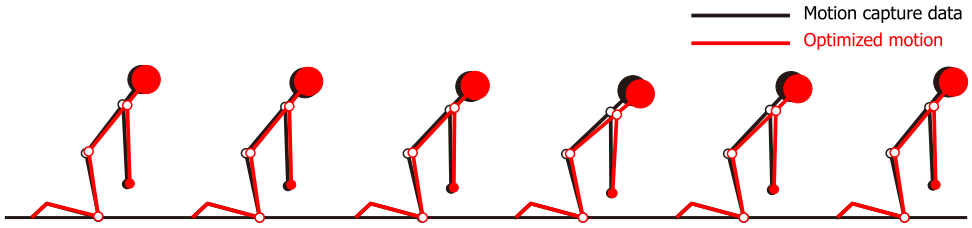

Fig. 11 Skilled motion and optimized motion

(same as Fig.8) and the red line represents the optimized motion. These motions are almost same, which means the skilled motion performed by the emergency life guard has been already optimized. A beginner's motion is also captured and optimized. The comparison of the body characteristic between the emergency life guard and the beginner is shown in Fig.12. The black line shows the emergency life guard and the red line shows the beginner. The beginner has a longer trunk and shorter arm with 60.0kg weight. Figure 13 shows the captured motion (black line) and optimized motion (red line), and Fig.14 shows time sequence data of τ_1 (knee joint), τ_2 (hip joint) and τ_3 (shoulder joint). The black dashed line shows an original torque which is calculated by inverse dynamic analysis based on the captured data. The red solid line shows the optimized torque. It is the first time for him to perform the chest compression. Even though he is received guidance from the emergency life guard in advance, his knee position *i.e.* x_0 is not appropriate. He takes a droopy posture and large torque is required. On the other hand, the optimization yields appropriate x_0, kinematic posture and dynamic motion, and the generative torque changes much smaller. Moreover, in the original motion, because the compression of the chest is not released, in other word, the constraint in Eq. (9) is not satisfied, the beginner's chest compression in not appropriate (it is cleared from the motion capture data). By the optimization, the chest compression is modified.

On the other hand, the body weight is an important element for the appropriateness of the chest compression. Figure 15 shows the difference of the optimized motion for a human with 60kg (red line) and 42kg (blue line) weight. The body heights of these persons are same. This results show that the difference of the body weight changes the appropriate x_0, and the distance between the position of the knee and the victim has to be appropriately instructed in the training session.

[DOI: 10.1299/mej.15-00155]

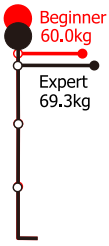

Fig. 12 Body comparison

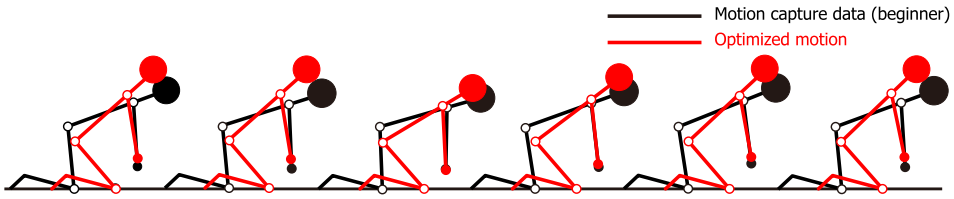

Fig. 13 Beginners motion and optimized motion

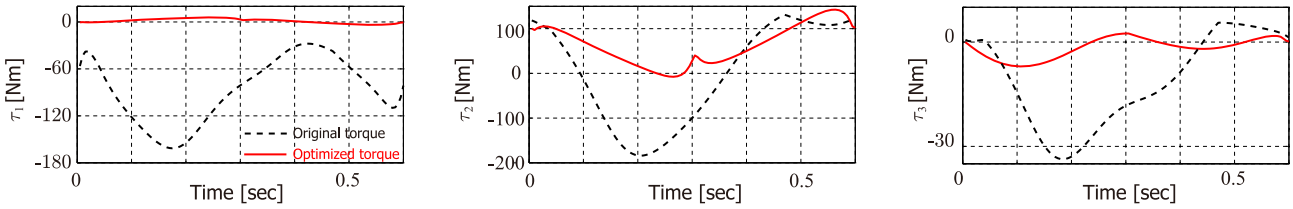

Fig. 14 Torque variety of beginners motion (captured data and optimized data)

4.2. Temporal optimization

The importance of the optimization of temporal redundancy is discussed in Sect. 2.3.2. However, the change of n as shown in Fig.6 causes the change of θ_{1i} $(i = 1, 2, \cdots N)$. Figure 16(a) shows an example for modification of n. When n is changed, all of y_{hi} are changed based on the optimization procedure. And it causes the change of θ_{1i}. Because N is a large number, there are so many design parameters in the proposed method. The larger change of the design parameter takes the longer time for convergence. Moreover, because n is an integer, the compression time takes discrete. In this paper, the temporal optimization is executed as shown in Fig,16(b). The sampling time T is changed to T_1 for the data number from 1 to n, and T_2 from $n+1$ to N. The design parameter is T_1 for the temporal optimization and T_2 is obtained by:

$$T_2 = \frac{TN - T_1 n}{N - n} \tag{43}$$

By this method, the value of θ_{1i} is not changed.

The change of the sampling time requires the modification of the optimization procedure. T_1 does not cause the change of θ_{1i} but $\dot{\theta}_{1i}$ and $\ddot{\theta}_{1i}$. Equations (16) and (17) are modified as follows.

$$\dot{\Theta} = \Theta \hat{F}^1, \quad \hat{F}^1 = \hat{\boldsymbol{G}}^1 R \hat{\boldsymbol{G}}^0 R \tag{44}$$

$$\ddot{\Theta} = \Theta \hat{F}^2, \quad \hat{F}^2 = -\hat{\boldsymbol{G}}^1 R \hat{\boldsymbol{G}}^1 R \tag{45}$$

$$\hat{\boldsymbol{G}}^k = \begin{bmatrix} \hat{g}^k_{11} & \hat{g}^k_{1N} & \cdots & \hat{g}^k_{12} \\ \hat{g}^k_{2N} & \hat{g}^k_{2\,N-1} & \cdots & \hat{g}^k_{21} \\ \vdots & \vdots & & \vdots \\ \hat{g}^k_{N2} & \hat{g}^k_{N1} & \cdots & \hat{g}^k_{N3} \end{bmatrix} \quad (k = 0, 1) \tag{46}$$

where $\hat{g}^k_{i*}$ is an impulse response of Eq. (14) defined by;

$$\hat{\boldsymbol{g}}^k_1 = \left\{ \overbrace{\hat{g}^k_{11}}^{T_1} \underbrace{\hat{g}^k_{12} \quad \cdots \quad \hat{g}^k_{1\,N-n+1}}_{T_2} \overbrace{\hat{g}^k_{1\,N-n+2} \quad \cdots \quad \hat{g}^k_{2N}}^{T_1} \right\} \tag{47}$$

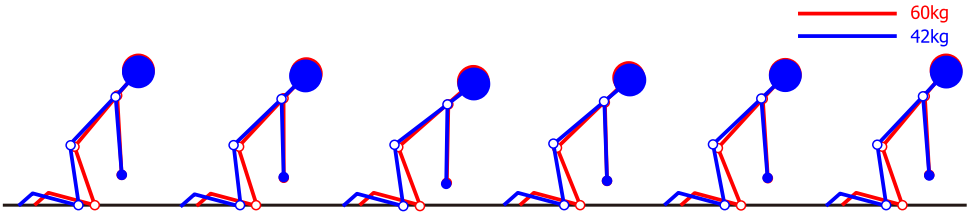

Fig. 15 Optimized chest compressions for 60kg (red line) and 42kg (blue line) weight

[DOI: 10.1299/mej.15-00155]

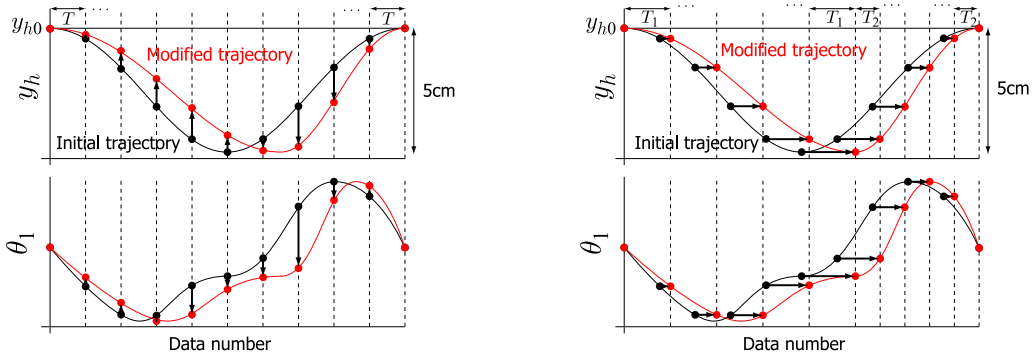

(a) Change of θ_1 with respect to chage of n (b) Change of the sampling time

Fig. 16 Example of temporal optimization

$$\hat{\boldsymbol{g}}_2^k = \left\{ \underbrace{\hat{g}_{21}^k \quad \hat{g}_{22}^k \quad \cdots \quad \hat{g}_{2\,N-n}^k}_{T_2} \quad \overbrace{\hat{g}_{2\,N-n+1}^k \quad \cdots \quad \hat{g}_{2N}^k}^{T_1} \right\} \tag{48}$$

$$\vdots$$

$$\hat{\boldsymbol{g}}_{N-1}^k = \left\{ \overbrace{\hat{g}_{N-1\,1}^k \quad \hat{g}_{N-1\,2}^k \quad \hat{g}_{N-1\,3}^k}^{T_1} \quad \underbrace{\hat{g}_{N-1\,4}^k \quad \cdots \quad \hat{g}_{N-1\;N-n+3}^k}_{T_2} \quad \overbrace{\hat{g}_{N-1\;N-n+4}^k \quad \cdots \quad \hat{g}_{N-1\;N}^k}^{T_1} \right\} \tag{49}$$

$$\hat{\boldsymbol{g}}_N^k = \left\{ \overbrace{\hat{g}_{N1}^k \quad \hat{g}_{N2}^k}^{T_1} \quad \underbrace{\hat{g}_{N3}^k \quad \cdots \quad \hat{g}_{N\;N-n+2}^k}_{T_2} \quad \overbrace{\hat{g}_{N\;N-n+3}^k \quad \cdots \quad \hat{g}_{NN}^k}^{T_1} \right\} \tag{50}$$

where T_1, T_2 represent sampling time on each data.

The gradient of J with respect to T_1 is obtained by;

$$\nabla_{T_1} J = \sum_{i=1}^{N} \left(\frac{\partial J}{\partial \dot{\theta}_{1i}} \frac{\partial \dot{\theta}_{1i}}{\partial T_1} + \frac{\partial J}{\partial \ddot{\theta}_{1i}} \frac{\partial \ddot{\theta}_{1i}}{\partial T_1} \right) \tag{51}$$

and T_1 is updated by;

$$T_1 \leftarrow T_1 + \delta \left(w_{T_1} \nabla_{T_1} J \right) \tag{52}$$

where w_{T_1} is a weighting parameter. Here we remark that because the impulse response of G^0 is represented by;

$$g^0(t) = F \exp(-Ft) \tag{53}$$

in the continues time domain,

$$\frac{\partial \dot{\Theta}}{\partial T_1} = \Theta \frac{\partial \hat{F}^1}{\partial T_1} \tag{54}$$

$$\frac{\partial \hat{F}^1}{\partial T_1} = \frac{\partial \hat{\boldsymbol{G}}^1}{\partial T_1} R \hat{\boldsymbol{G}}^0 R + \hat{\boldsymbol{G}}^1 R \frac{\partial \hat{\boldsymbol{G}}^0}{\partial T_1} R \tag{55}$$

is easily calculated. And $\partial \ddot{\Theta} / \partial T_1$ is obtained by the same way.

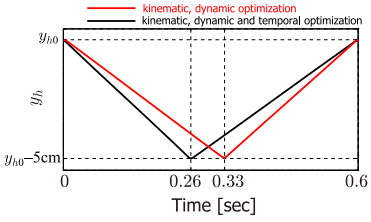

Fig. 17 Change of y_h by temporal optimization

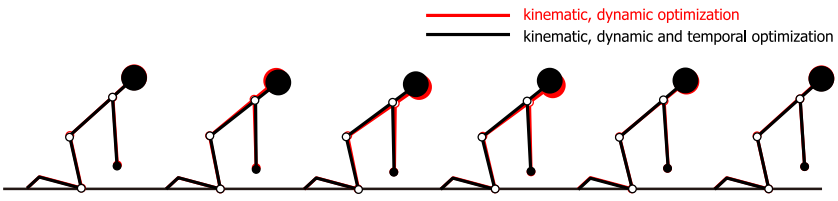

Fig. 18 Motion change by the appropriate compressing time

[DOI: 10.1299/mej.15-00155]

The motion in Fig.15 with 60kg weight (red line) is kinematically, dynamically and temporally optimized. Figure 17 shows the time variety of y_h. Motion period is 0.6sec which is not changed and the compressing time is 0.33sec. On the other hand, the compressing time is changed to 0.26sec. Figure 18 shows a kinematically and dynamically optimized motion which is same as Fig.15 (red line) and kinematically, dynamically and temporally optimized motion (black line).

5. Optimization of motion aid

5.1. Motion aid for the chest compression

It is important that the chest compression is widely known in public. There are sometimes only an elderly person and a child are in their home. In case of emergency, the child has to make the chest compression. In these days, a basic life-saving certification for elementally school students is conducted. It is said that 35kg body weight is required for the chest compression. The chest compression of a child with 37kg body weight and 139.5cm body height is optimized. The torque varieties of each joint in the optimized motion are shown in Fig.19. It requires very large torque, between 0.2sec

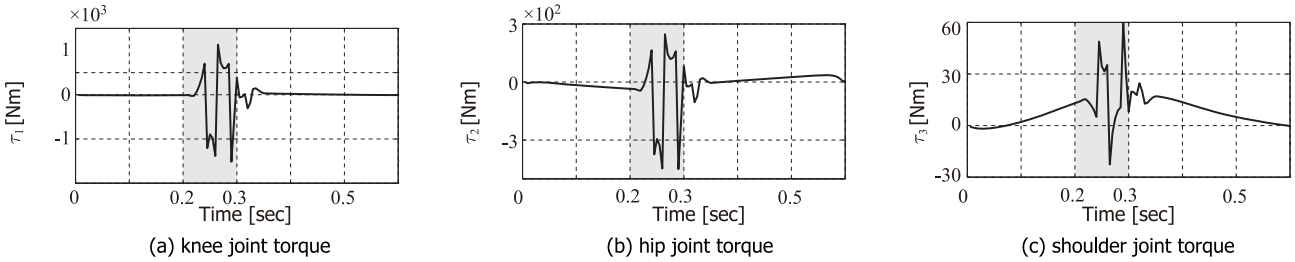

Fig. 19 Torque variety of the optimized chest compression with 37kg body weight

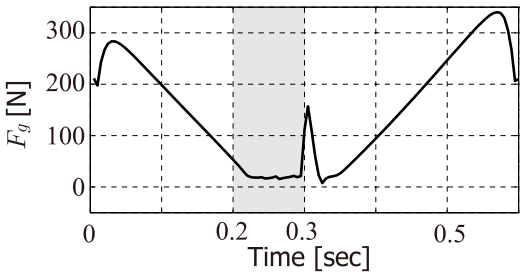

Fig. 20 Ground force of chest compression

and 0.3sec, which is because the constraint of $F_g > 0$ in Eq. (8). Figure 20 shows the time variety of the ground force. To keep the ground force positive between 0.2sec and 0.3sec, a large joint torques are required.

The reason of this result is that the body weight is too small to make the chest compression. However, by using a mass that supports the small body weight as shown in Fig.21, the children will make the appropriate chest compressions. The dynamical model is represented by Fig.22. The purpose of this section is to design an appropriate mass with respect to the body weight.

Fig. 21 First-aid chest compression with a weight

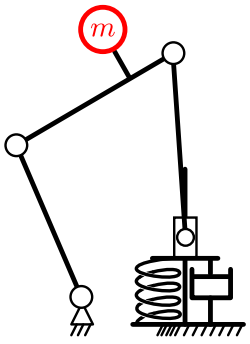

Fig. 22 Dynamical model of chest compression with a motion aid

[DOI: 10.1299/mej.15-00155]

5.2. Optimization of motion aid

As the same procedure in Sect. 3, the weight of mass m is optimized. The gradient of J with respect to m is simply obtained by:

$$\nabla J_m = \frac{\partial J}{\partial m} \tag{56}$$

Figure 23 shows the relationship between the optimal mass and body weight, and Fig.24 shows the value of J with respect to body weight with/without the optimal mass. These results show that the performer whose weight is less than 50kg

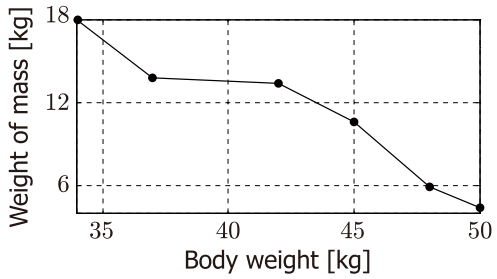

Fig. 23 Optimal weight with respect to body weight

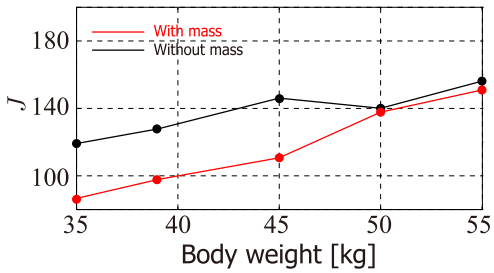

Fig. 24 Relationship between J and body weight

requires the motion aid. The main reason is that the constraint in Eq. (8) (ground force should be positive) is not satisfied because of the light body weight. Through the optimization procedure, the design parameters are changed so that the constraints are satisfied, which sometimes leads the larger value of J. An elementally school student whose weight is about 38kg (average of 11 years old child) will make the chest compression easily with 14kg mass. Figure 25 shows the motion of the optimized chest compression of 42kg child with/without the optimal mass. The black line shows without

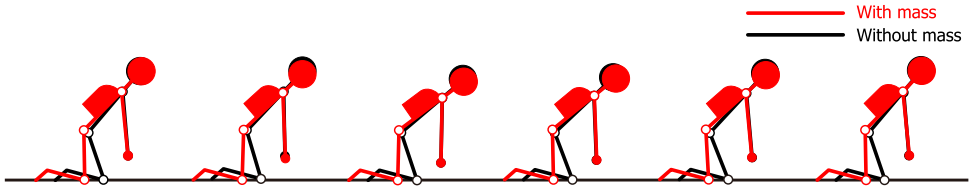

Fig. 25 Optimal motion for 42kg body weight with/without the optimal mass

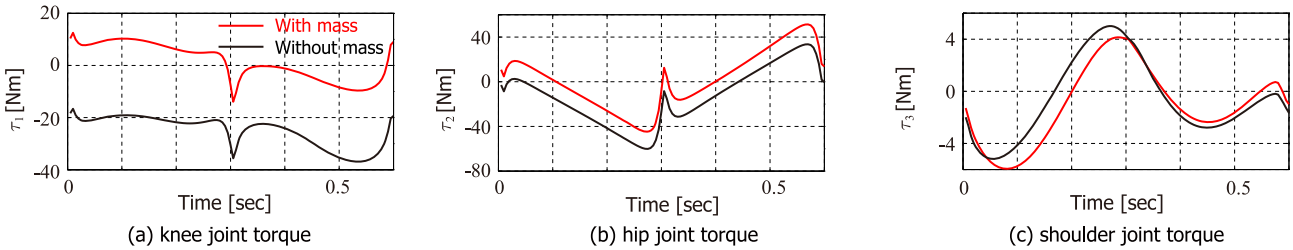

Fig. 26 Torque variety of the optimized chest compression with/without the mass

mass, the red line shows with the optimal mass. The inertia force of the mass is effectively utilized with the larger x_0. The time varieties of the torques are shown in Fig.26. The black line shows without mass, the red line shows with the optimal mass. By using the mass, the knee joint torque changes much smaller without increasing the hip and shoulder torques.

6. Evaluation of physical load by measuring heart rate

6.1. Measurement of heart rate

To evaluate the obtained motion, heart rate is measured to investigate the physical load of performers. The chest compressions of three performers (performer A, B and C) are motion captured, and their heart rate are also measured during the motion. Body parameters of performers are shown in Table 1. Other parameters such as link length are obtained from the capture data. The performer A is a beginner, the performer B and C are emergency life guards. The mass is optimized based on the body height and weight. Because the performers' body weights are less than 50kg, a mass is required for the appropriate chest compression. A weight jacket shown in Fig.27(a) is utilized for the mass. The weight

[DOI: 10.1299/mej.15-00155]

Table 1 Body parameters of performers

Performer	Body height [cm]	Body wight [kg]	Mass weight [kg]	Sex	Age
A	171	48	6.6	male	20's
B	156	46	7.0	female	50's
C	158	50	4.4	female	60's

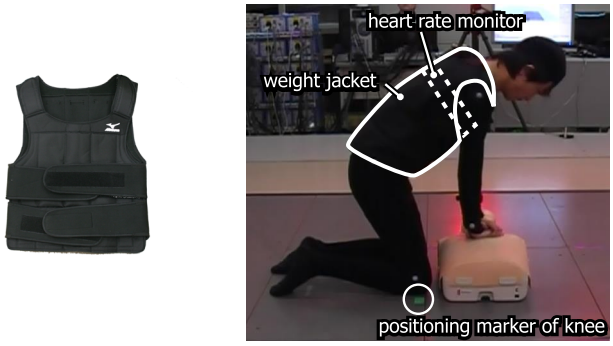

(a) weight jacket (b) chest compression with a weight jacket

Fig. 27 Chest compression with a mass (weight jacket)

of the jacket is adjustable by putting small weights in the pockets. A performer making the chest compression is shown in Fig.27(b). He wears the jacket, and a heart rate monitor is set on his chest.

The optimal motion is displayed by the movie to the performer a priori. The position of the knee (x_0) and initial posture are well instructed. Figure 28 shows the measured heart rate. The solid line shows with a mass, and the dashed

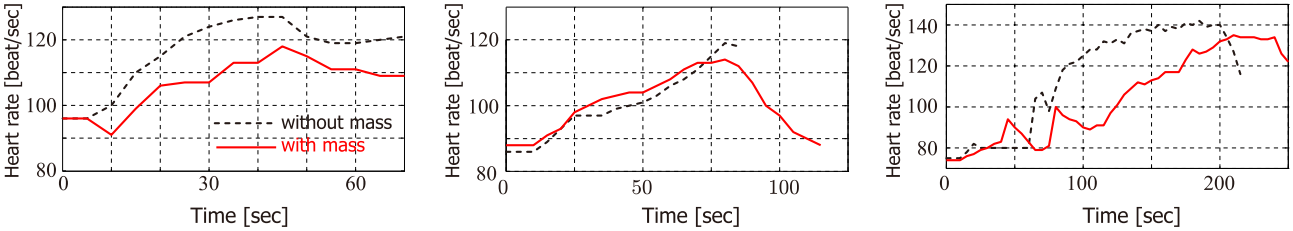

Fig. 28 Heart rate during the chest compression

line shows without a mass for comparison. The sampling time of the measurement is 5sec. These figures show that

(1) By using the optimal mass, the physical load changes smaller for the performers A and C even though they carry a heavy weight on their shoulder. It shows the effectiveness of the motion aid.

(2) The physical load for the performer B does not change even though she uses the optimal mass. The reason may be that she is an active emergency life guard and she has already acquired her best style of the chest compression.

7. Conclusions

In this paper, focusing on the chest compression, we have derived a motion optimization method considering kinematic redundancy, dynamical redundancy and temporal redundancy. The results are summarized as follows;

- Human dynamic model of the chest compression is derived as a link model considering constraints.
- To obtain the angular velocity and acceleration from the motion capture data, pseudo-differential and zero-phase filter are introduced. Because of the benefit of this method, the relationship between angle data and angular velocity/acceleration is represented by a product of the angle data and a constant matrix.
- Based on an objective function, the optimization method of the chest compression is derived, and its effectiveness is evaluated by simulations.
- An optimization method of the temporal redundancy is proposed by changing the sampling time of the data sequence.
- It is cleared that a human who has light body weight is difficult to make the chest compression because of the

[DOI: 10.1299/mej.15-00155]

constraint of the positive ground force. And a motion aid with a mass is proposed and optimized.

- The effectiveness of the proposed method is evaluated by measuring the heart rate of the performer from physical load point of view.

Acknowledgment

This research is supported by JSPS Grants-in-Aid for Scientific Research (Category: Grant-in-Aid for Challenging Exploratory Research) entitled 'Optimization of Chest Compression for Basic Life-saving Certification of Elementary School Students'.

References

Abellaa, B. S., Edelsonb, D. P., Kim, S., Retzerc, E., Myklebustd, H., Barryc, A. M, O'Hearn, N., Vanden Hoek, T. L. and Beckera, L. B., CPR quality improvement during in-hospital cardiac arrest using a real-time audiovisual feedback system, Resuscitation, Vol.73, Issue 1, (2007), pp.54–61.

Boyle, A. J., Wilson, A. M., Connelly, K., McGuigan, L., Wilson, J. and Whitbourn, R., Improvement in timing and effectiveness of external cardia compressions with a new non-invasive device: the CPR-Ezy, Resuscitation, Vol. 54, Issue 1, (2002), pp.63–67.

Field, J. M., Hazinski, M. F., Sayre, M. R. et. al., 2010 American Heart Association Guidelines for CPR and ECC, American Heart Association 2010, (2010).

Hollerbach, J. M. and Suh, K. C., Redundancy Resolution of Manipulators through Torque Optimization, IEEE Journal of Robotics and Automation, Vol.RA-3, No.4, (1987), pp.308–316.

Khoury, A. E., Lamiraux, F., and Taïx, M., Optimal Motion Planning for Humanoid Robots, 2013 IEEE International Conference on Robotics and Automation, (2013), pp.3136–3141.

Kim, J. H., Optimization of throwing motion planning for whole-body humanoid mechanism: Sidearm and maximum distance, Mechanism and Machine Theory, Vol. 46, Issue 4, (2011), pp.438–453.

Kim, S. and Park, F. C., Fast Robot Motion Generation Using Principal Components: Framework and Algorithms, IEEE Transactions on Industrial Electronics, Vol.55, No.6, (2008), pp.2506–2516.

Okada, M. and Kayashima, S., Motion Instruction of First Aid Chest Compression using Pseudo-reference and Its Evaluation, Transaction of the Japan Society of Mechanical Engineering Series C, Vol. 79, No. 800, (2013), pp.1090–1101, (in Japanese).

Wang, C. E., Timoszyk, W. K. and Bobrow, J. E., Payload Maximization for Open Chained Manipulators: Finding Weightlifting Motions for a Puma 762 Robot, IEEE Transactions on Robotics and Automation, Vol.17, No.2, (2001), pp.218–224.

Wang, J. M., Hammer, S. R., Delp, S. L. and Koltun, V., Optimizing Locomotion Controllers Using Biologically-Based Actuators and Objectives, ACM Transactions on Graphics, Vol.31, No.4, (2012), (Proc. of SIGGRAPH 2012)

[DOI: 10.1299/mej.15-00155]